
A MISCLASSIFICATION NETWORK-BASED METHOD FOR COMPARATIVE GENOMIC ANALYSIS

Wan He

Northeastern University, Boston, MA, USA
 he.wan1@northeastern.edu

Tina Eliassi-Rad

Northeastern University, Boston, MA, USA
 Santa Fe Institute, Santa Fe, NM, USA
 t.eliaassirad@northeastern.edu

Samuel V. Scarpino

Northeastern University, Boston, MA, USA
 Santa Fe Institute, Santa Fe, NM, USA
 Vermont Complex Systems Institute, University of Vermont, Burlington, VT, USA
 s.scarpino@northeastern.edu

ABSTRACT

Classifying genome sequences based on metadata has been an active area of research in comparative genomics for decades with many important applications across the life sciences. Established methods for classifying genomes can be broadly grouped into sequence alignment-based and alignment-free models. The more conventional alignment-based models rely on genome similarity measures calculated based on local sequence alignments or consistent ordering among sequences. However, these alignment-based methods can be quite computationally expensive when dealing with large ensembles of even moderately sized genomes. In contrast, alignment-free approaches measure genome similarity based on summary statistics in an unsupervised setting and are computationally efficient enough to analyze large datasets. However, both alignment-based and alignment-free methods typically assume fixed scoring rubrics that lack the flexibility to assign varying importance to different parts of the sequences based on prior knowledge and also that prediction errors are random with respect to the underlying data generating model. In this study, we integrate artificial intelligence and network science approaches to develop a comparative genomic analysis framework that addresses both of these limitations. Our approach, termed the Genome Misclassification Network Analysis (GMNA), simultaneously leverages misclassified instances, a learned scoring rubric, and label information to classify genomes based on associated metadata and better understand potential drivers of misclassification. We evaluate the utility of the GMNA using Naive Bayes and convolutional neural network models, supplemented by additional experiments with transformer-based models like Enformer [13], to construct SARS-CoV-2 sampling location classifiers using over 500,000 viral genome sequences and study the resulting network of misclassifications. We demonstrate the global health potential of the GMNA by leveraging the SARS-CoV-2 genome misclassification networks to investigate the role human mobility played in structuring geographic clustering of SARS-CoV-2 and how genomes were misclassified by our model.

1 Introduction

Artificial Intelligence (AI) based approaches, e.g., models using deep learning architectures, have demonstrated remarkable accuracy in classifying genome sequencing data according to metadata such as geographic sampling location [79, 30], drug resistance [29, 111, 59], taxonomic grouping [74, 73, 35], and various other phenotypes of interest [12, 97, 49]. Despite the impressive performance of these models, they typically rely on the widely held assumption in machine learning/AI that classification accuracy best reflects model performance [20]. As a consequence, such AI-based genome comparative methods can likely be enhanced by studying drivers of misclassification. The reason-

ing is that, while ML/AI approaches typically assume errors are driven by random noise inherent in the data, i.e., aleatoric uncertainty, in many biological settings misclassifications are driven by model formulation errors or incomplete representation of the biological system, i.e., epistemic uncertainty. Instead of viewing this epistemic challenge as a weakness, we see an opportunity to derive insights from studying how genomes are misclassified by AI models.

Here, we introduce the Genome Misclassification Network Analysis (GMNA), a genome association analysis framework that extends beyond classification accuracy to extract knowledge from the pairwise relationships among misclassified data. By acknowledging and utilizing the pairwise relationships among the misclassified data, our framework generates additional insights into the underlying processes giving rise to the misclassified genomic data. This framework further allows us to integrate network-science-based approaches into downstream analysis of the drivers of misclassification. We believe the use of the GMNA may provide meaningful insights beyond traditional accuracy-based approaches across the broader field of comparative genomics and for non-genetic data coming from varying application domains.

Comparative genomics: Comparative genomics enhances our understanding of the functional and/or evolutionary significance of genetic variation by analyzing sequences from different individuals and/or species [100, 33, 71, 3, 39, 53]. Among comparative genomics approaches, alignment-based methods such as variants of BLAST [6, 93, 50] and CLUSTAL [44, 99, 95] utilize dynamic programming algorithms minimizing edit distance [76, 96] to search for aligned sub-sequences. However, such alignment-based methods, which assume collinearity, are limited in capturing higher-order information such as non-linear relationships between subsequences and structural rearrangements within sequences [102, 116]. Moreover, finding the optimal alignment is a combinatorial optimization problem that does not have a continuous solution space to allow for a gradient descent-based optimization scheme [54, 22], although prior work suggests alignments based on approximate edit distances should exhibit favourable runtime scaling [16]. Nevertheless, even finding an approximately optimal solution can be computationally infeasible when dealing with even moderate numbers of moderately sized sequences [10, 14, 88]. Alternatively, graph-based alignment methods [51, 52] have improved the efficiency and accuracy of aligning whole-genomes, particularly in the highly polymorphic genomic regions. These methods encode genomic sequences as graphs, wherein long, identical subsequences are represented as vertices [7]. However, this class of methods still faces the challenge of scalability and aligning highly divergent sequences [72]. Unlike alignment-based methods, alignment-free comparative approaches in genomics typically rely on statistics derived from K-mer words [18, 89, 103] to capture key features without the need for sequence alignment and are therefore efficient for large-scale genome comparisons. Despite the computational benefits of alignment-free approaches, sequence ordering (including interaction effects) beyond length k cannot be modelled by the most K-mer statistics [116].

Applications of deep learning to genomics with examples from SARS-CoV-2: Deep learning techniques, particularly language models that process sequence data, have significantly impacted genomics-based research [34, 78]. Here, very high-dimensional models are trained to identify the underlying patterns in genomic data and have demonstrated impressive performance in downstream tasks such as motif discovery [27], promoter region identification [112, 46], non-coding variant prediction [115], protein-ligand binding predictions [26], and gene expression prediction [13]. Among these advancements, transformer-based generative models [101, 31], such as DNABERT [46], BigBird [112], and Enformer [13] achieved state-of-the-art performance in many applications by integrating long-range interactions through their attention mechanism. However, their training is extremely computationally intensive and constrained by token length. As an example, BERT is quadratically dependent on input sequence length and has a maximum token limit of 512—note that the SARS-CoV-2 genome (which is comparatively small) comprises over 30,000 bases. As a result, SARS-CoV-2 genome sequences cannot be fed into BERT without truncation or serious compression due to their length. While BigBird [112] introduced a block-sparse attention mechanism to reduce complexity to a linear dependency on length, its 4096 token limit still falls short of addressing the full extent of whole genomes. Despite these challenges, AI-driven approaches have been employed to study SARS-CoV-2 in applications such as evolution prediction and lineages identification [104, 21] SARS-CoV-2 virus identification [67, 43], drug repurposing and prediction [84, 47, 55, 17], diagnosis and treatment [1].

Genome Misclassification Network Analysis: Here, we introduce an alignment-free framework for comparative analysis, which we call the Genome Misclassification Network Analysis (GMNA). The GMNA measures associations between ensembles of genome sequences based on the empirical likelihood of their misclassification. The discriminative filters used to compare the genome ensembles are learned by an arbitrary AI model using genome feature information. Briefly, the GMNA starts with a trained classifier that takes as input a genome sequence and predicts metadata of interest. We then construct a weighted misclassification network using the misclassified instances, where nodes represent ensembles of genome sequences from different metadata classes. Edges indicate associations between pairs of genome sequence ensembles, with weights representing "indistinguishability" scores derived from empiri-

cal misclassification likelihoods between ensembles from distinct metadata classes. By selecting specific features of interest, pairwise associations among genome sequences with different realizations of these feature variables can be explored. GMNA offers a computationally efficient comparative genomics tool for studying associations between large ensembles of genome sequences while leveraging valuable label information.

To address limitations of the alignment-based comparative genomics approaches, instead of attempting to explicitly design a quantity to measure the association among genome sequences, we propose a framework that could use any arbitrary AI model to learn discriminative features and quantify the association between ensembles of genome sequences. Under this AI-based misclassification network framework, we rely on the judgement of the machine to determine how close a pair of genome ensembles are by computing an *indistinguishability* score, based on the empirical misclassification likelihood. The GMNA framework hypothesizes that—given a decent classifier—misclassification happens when the predicted class and the true class of the sequences shared sufficient distinctive features and therefore are *indistinguishable* enough to deceive the AI to misidentify the input sequences.

Without manual feature engineering or explicitly specifying a feature selection scheme for the genome classification task, the AI model automatically learns the features that optimize performance. Consequently, using the AI framework also has the added benefit of incorporating target output, i.e., the class labels, in the feature mining process. Moreover, this framework offers flexibility in the choice of the appropriate AI model. The classification model could be tailored to suit the specificity of the learning problem. For instance, a binary genome sequence classification problem can be accurately solved with nearly 100% accuracy using a convolutional neural network. However, under computation resource constraints especially for more complex tasks, such as fine-grained sequence classification on longer sequences, a Naive Bayes model may be a more efficient choice. We emphasize that the purpose of this study is not to advance a specific model’s classification performance on whole genome sequence, but to offer an alternative and efficient approach for genome ensemble comparative analysis based on the often overlooked misclassified instances.

To demonstrate the utility of the GNMA, we utilized 551,230 labeled whole genome SARS-CoV-2 sequences, where each label denotes the specific region in which the sequence was collected. We used CNN and Naive Bayes as the backbone methods of our framework. With spatial sampling location predictions from these trained classifiers, we compared the learned misclassification network with a flights network from Official Airline Guide (OAG) to study how travel impacts genome variation. Finally, we discuss how our GMNA may be applied to datasets labeled with multiple features.

Contributions

The key contributions of this work are as follows:

- We introduce a novel alignment-free framework, termed the Genome Misclassification Network Analysis (GMNA), that uses empirical misclassification likelihoods to measure associations between ensembles of genome sequences.
- We identify the pairwise association between the target outcome and the predicted outcome, which is then utilized to design a data-driven framework that can incorporate any arbitrary AI model for use in comparative genome analysis.
- We propose the concept of *indistinguishability* as a metric to quantify the association between pairs of genome groups, which captures the genetic diversity and complexity of genome ensembles.
- Our framework is adaptable and can incorporate any AI model for comparative genome analysis, making it applicable across various genomic datasets and features.
- Using more than 500,000 SARS-CoV-2 genomes, we demonstrate that GMNA can uncover geographic associations between genome sequences with limited computational resources.
- We construct a misclassification-based network and compare it with the Official Airline Guide (OAG) flights network, highlighting how human activities, such as global transportation, impact genome variation and evolution.
- We introduce the leave-one-class-out (LOCO) model to balance the trade-off between generating sufficient misclassified data for association inference and maintaining model credibility with high prediction accuracy.
- Our framework provides a computationally efficient tool for large-scale comparative genomics, offering insights into phylogenetic structure and evolutionary patterns.

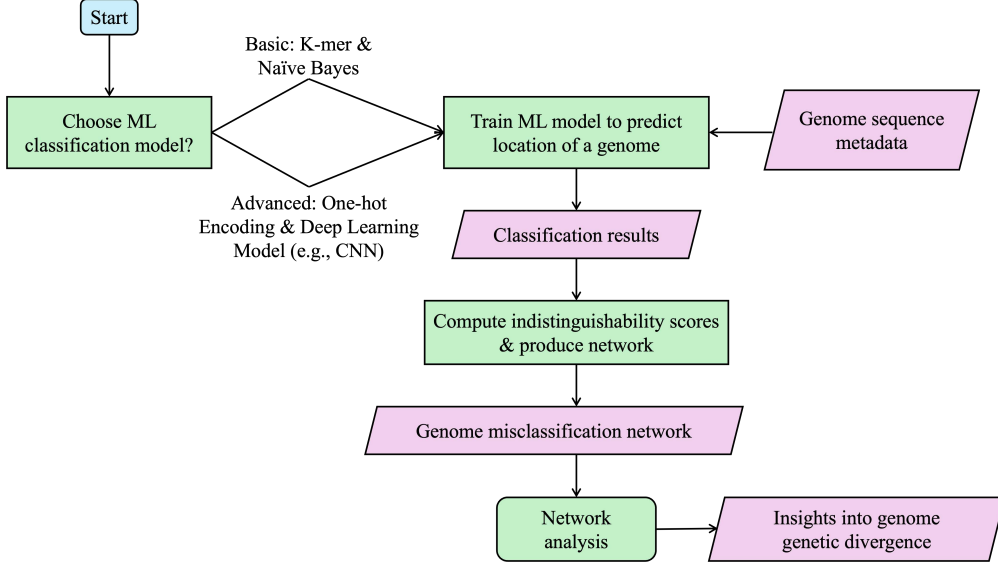


Figure 1: Flowchart of the Genome Misclassification Network Analysis Framework.

2 Genomic Misclassification Network Analysis (GMNA)

We designed an integrative procedure that combines AI and methods from network science to perform comparative genomic analysis. We first solved a genome sequence classification problem, mapping genome sequences to metadata. The misclassified instances outputted from the classifying machine are then utilized to compute *indistinguishability* scores that measure pairwise associations among genome groups for correlation-based analysis. We interpret the edges in this genomic misclassification network as the association between ensembles of genome sequences under the assumption that genomes with more shared discriminative latent features—and thus fewer divergent features—are more likely to confuse the machine and mislead it into making mistakes. In other words, the more *indistinguishable* a pair of genome classes appears to the trained AI, the more similar the two classes are. For example, if we are trying to predict spatial sampling location, we set the target class labels to be regions where genome sequences were collected. A misclassification network can then be constructed from the classification results, where nodes are the genome collection regions, and an edge between region A and region B is established when a genome from region A is incorrectly classified as being from region B.

More generically, each node in a misclassification network represents data of a specific class where each class is one of the instances in the target label set \mathcal{Y} . The target set \mathcal{Y} for the classifier to predict is chosen to be the attribute of which the association among the instances is the subject of research interest. Associations between any pair of data ensembles labeled by class instances (c_i, c_j) of the attribute of research interest \mathcal{Y} are measured by how indistinguishable these data points are to the classifying machine. The more indistinguishable the data labeled by these two classes appears to the AI, the more similar we can assume the classes to be. Formally, the weight w_{ij} of edge e_{ij} in the misclassification network, interpreted as the association between class c_i and $c_j \in \mathcal{Y}$, is given by the *indistinguishability* score between data ensembles \mathcal{X}_i and \mathcal{X}_j , where $\mathcal{X}_i = \{x \in \mathcal{X} : y(x) = c_i\}$, computed as the symmetrized empirical probability of misclassification, as shown in Equation 2. When applied to genomic data we call our framework, the Genome Misclassification Network Analysis (GMNA). Despite focusing on genomic data for the remainder of the paper, we stress that the underlying methodology is quite general and can be readily extended to non-genomic data.

The selection of suitable AI models within the GMNA framework depends on the complexity of the classification problem at hand and resolution of the metadata. For example, a challenging aspect of classifying SARS-CoV-2 whole genome sequences is the high computational cost associated with their length. SARS-CoV-2 genomes are around 35,000 bases and are composed of a very small vocabulary of 16 base letters, which includes degenerate bases. The long length relative to vocabulary size makes it critical for the classifier to account for combinations, permutations, local context, and long-range interactions among subsequences, as genome sequences exhibit a highly context-sensitive structure. To capture the essential subsequence patterns within the genomic data, we adopted K-mer preprocessing coupled with Naive Bayes as a baseline approach for GMNA. The K-mer preprocessing allowed the expansion of the vocabulary used in genome sequence analysis and thus increased the diversity of features considered while incorporating local context. This choice was also motivated by the method’s computational efficiency, which

remains independent of the sequence length or the number of sequences. Importantly, this independence allows us to efficiently measure associations between large ensembles of lengthy genome sequences, making our approach robust and scalable. To enhance the classifier’s performance, we employed a convolutional neural network (CNN) architecture. The CNN reduces sequence length while learning filters to extract label-specific, discriminative features from the genomes, enabling efficient and automatic feature extraction.

The resulting misclassification network could then be further analyzed using any network analysis techniques to study its network properties of interest. For instance, it could be fed to any community detection algorithms [40, 110, 42, 62, 38] to evaluate how data with different attributes of interests are associated. Alternatively, nodes, i.e. genome ensembles, could be characterized based on any centrality measure such as betweenness [77] or page-rank [80].

2.1 Misclassification Network Construction

2.1.1 Problem definition

To obtain the pair-wise associations based on *indistinguishability* scores from the misclassification results, we consider the classification problem of mapping a set of N genome sequences $\mathcal{X} = \{x_1, \dots, x_N\}$ to their location labels $\mathcal{Y} = \{loc(x_1), \dots, loc(x_N)\} = \{y_1, \dots, y_N\} = \{r_1, \dots, r_K\}$. Here, K represents the cardinality of the label set \mathcal{Y} . We define \mathcal{X}_{r_i} as genomes originating from region r_i , where $r_i \in \mathcal{Y}$ and $\mathcal{X}_{r_i} = \{x_m \mid y_m = r_i, m \in \{1, \dots, N\}\}$. Denote $E_f(r_i, r_j)$ as the event of a classifier f incorrectly classifying a genome sequence from region i to region j . Denote $\mathcal{C}_f(\mathcal{D}_s, r_i, r_j)$ as the count of occurrences of event $E_f(r_i, r_j)$ where $r_i, r_j \in \mathcal{Y}$ when input data \mathcal{D}_s is used for predictions. Formally, $\mathcal{C}_f(\mathcal{D}_s, r_i, r_j) = \sum_{x \in \mathcal{X}_{r_i} \subseteq \mathcal{D}_s} I(f(x) = r_j \mid y(x) = r_i)$. The empirical probability of sequences from region r_i being misclassified as from region r_j by classifier f is calculated as $P_f(\mathcal{X}_{r_i}, r_i, r_j) = \frac{\mathcal{C}_f(\mathcal{X}_{r_i}, r_i, r_j)}{|\mathcal{X}_{r_i}|}$. The objective function for classifier training is to minimize the total misclassification cost:

$$\sum_{x \in \mathcal{X}} cost(f(x), y(x)). \quad (1)$$

We summarized our notation in Table 1.

Table 1: Notation Table

Symbol	Description
N	Total number of genome sequences
K	Cardinality of the label set \mathcal{Y}
\mathcal{X}	Set of N genome sequences, $\mathcal{X} = \{x_1, \dots, x_N\}$
\mathcal{Y}	Set of location labels, $\mathcal{Y} = \{loc(x_1), \dots, loc(x_N)\} = \{y_1, \dots, y_N\} = \{r_1, \dots, r_K\}$
\mathcal{X}_{r_i}	Set of genomes originating from region r_i , where $r_i \in \mathcal{Y}$ $\mathcal{X}_{r_i} = \{x_m \mid y_m = r_i, m \in \{1, \dots, N\}\}$
$E_f(r_i, r_j)$	Event of classifier f incorrectly classifying a genome sequence from region i to region j
$I(f(m) = r_j \mid y(m) = r_i)$	Indicator function evaluating to 1 if classifier f predicts r_j given that the true label is r_i for genome sequence m , otherwise 0
$\mathcal{C}_f(\mathcal{D}_s, r_i, r_j)$	Count of occurrences of event $E_f(r_i, r_j)$ when input data \mathcal{D}_s is used for predictions $\mathcal{C}_f(\mathcal{D}_s, r_i, r_j) = \sum_{m \in \mathcal{X}_{r_i} \subseteq \mathcal{D}_s} I(f(m) = r_j \mid y(m) = r_i)$
$P_f(\mathcal{X}_{r_i}, r_i, r_j)$	Empirical probability of sequences from region r_i being misclassified as from region r_j by classifier f $P_f(\mathcal{X}_{r_i}, r_i, r_j) = \frac{\mathcal{C}_f(\mathcal{X}_{r_i}, r_i, r_j)}{ \mathcal{X}_{r_i} }$

Our proposed Misclassification Network Analysis (MNA) framework can be applied under various setups. Below, we discuss a few options:

Binary Misclassification Network Analysis (MNA) Under the binary MNA setting, pairwise genome ensemble similarities are obtained by training a binary classifier for every pair of genome ensembles. The binary-classification setting computes the pairwise genome ensemble association between \mathcal{X}_{r_i} and \mathcal{X}_{r_j} using a training dataset containing only genome sequences from the two regions r_i and r_j . The association between any two ensembles is measured by the inverse of the classification accuracy of the binary classifier, as shown in Equation 2.

Multiclass MNA In the multi-class MNA setting, pairwise genome ensemble similarities are obtained by training a multiclass classifier (MCC) and aggregating the misclassified instances. Thus computation of inter-class associations among all pairs of data ensembles requires training only one classifier. For GMNA, the *indistinguishability* scores of all pairs of genome ensembles $\mathcal{X}_{r_i}, \mathcal{X}_{r_j}$ become available once the MCC model completes training and makes predictions on the test set.

Under both the binary and multiclass settings, the number of nodes for misclassification network analysis (MNA) is given by the order of the target variable set \mathcal{Y} , specifically $\mathcal{Y}_{train} \cap \mathcal{Y}_{test}$, that is the number of classes for prediction. For spatial analysis on the genome sequences, the target variable is the location information of the genomes; thus, each node represents genome sequences ensembled by the region labels. The *indistinguishability* score between genome ensemble \mathcal{X}_{r_i} and \mathcal{X}_{r_j} from classifier f is given by:

$$indistinguishability(\mathcal{X}_{r_i}, \mathcal{X}_{r_j}) = P_f(\mathcal{X}_{r_i}, r_i, r_j) + P_f(\mathcal{X}_{r_j}, r_j, r_i). \quad (2)$$

Leave-one-class-out (LOCO) MNA However, both the binary and MCC misclassification network analysis (MNA) schemes face a trade-off between prediction accuracy and having enough misclassified instances to establish meaningful correlations for inference. A high-performance classifier accurately categorizes genome sequences has the issue of not producing sufficient misidentified data for class-wise association inferences. To address this dilemma, we propose the leave-one-class-out (LOCO) misclassification generation scheme. Although in this work, our goal is not to eliminate all the incorrectly classified cases, since the purpose of this study is not to push classification accuracy, but rather to study the temporal and spatial associations among SARS-CoV-2 genome sequences based on the incorrectly classified cases. However, a poorly performing AI that frequently misidentifies the genome origins lacks credibility for further results analysis.

To resolve the dilemma between consistently generating more incorrectly classified data points for inference and maintaining satisfactory prediction accuracy, we introduced a leave-one-class-out (LOCO) model. This approach iteratively leaves out one class of genome sequences during the training process, and the model is subsequently trained to classify the excluded sequences, and is trained to later classify the genome sequences that were left out during training. The LOCO classifier appoints a "centroid" region and trains a classifier on a data subset that excludes genome sequences from this selected centroid region. This process iterates through the entire set of regions, with each region taking a turn as the centroid. After training, the leave-one-class-out classifier is applied to the genome sequences from the currently excluded centroid region. One major benefit of this setting is the guaranteed abundance of misclassified instances and thus greater statistical significance in general, since each genome from the centroid is inevitably misclassified into one of the remaining classes, as the training subset does not include the true target region (the centroid itself). This setting produces a star misclassification network, with the centroid as the hub and the degree of a node corresponding to the frequency of genome sequences from the centroid region getting misclassified as originating from the region corresponding to that node. Finally, the genome ensemble association between the centroid and the remaining regions could be computed as,

$$indistinguishability(\mathcal{X}_{centroid}, \mathcal{X}_{r_j}) = P_{LOCO}(\mathcal{X}_{centroid}, r_{centroid}, r_j) \quad (3)$$

For example, if the US is the appointed left-out "centroid" region, the leave-one-class-out classifier will be trained on the entire preprocessed dataset excluding the genome sequences from the US. During prediction, the test set will consist only of the US sequences, and the leave-one-class-out classifier will be used to map the US genomes to a non-US country. As a result, all the predictions made are incorrect and are used solely for correlational inference. Under this setting, which produces a consistent amount of incorrectly classified samples, improving the classification accuracy no longer limits the amount of data needed for the misclassification analysis.

Algorithm 2 LOCO Algorithm: This algorithm addresses the dilemma between the availability of misclassified instances for inference and maintaining prediction accuracy by purposefully generating misclassified instances.

Input:

$\mathcal{X}_{\text{centroid}} \in \{0, 1\}^{B \times L_{\max} \times N_{\text{centroid}}}$: One-hot encoded genomes from the centroid region, where B is the number of nucleotide bases, L_{\max} is the length of the longest genome, and N_{centroid} is the number of genomes in the centroid region

Output:

1. $f_{\text{LOCO}}^{\text{centroid}}$: Trained classifier for the centroid region
2. $\text{indistinguishability}(r_{\text{centroid}}, r')$: Association measure between centroid region and region r'

for all region r **do**

1. centroid region $r_{\text{centroid}} := r$
2. $\mathcal{X}_{\text{train}} := \mathcal{X}_{\text{train}} - \mathcal{X}_{\text{centroid}}$
3. Train classifier $f_{\text{LOCO}}^{\text{centroid}}$ that minimise $\sum_{x \in \mathcal{X}_{\text{train}}} \text{cost}(f(x), y(x))p(x)$

for all region $r' \neq r$ **do**

Compute "association" between genome ensembles from centroid region and region r' as:

$$\text{indistinguishability}(r_{\text{centroid}}, r') = \frac{\sum_{x_i \in \mathcal{X}_{\text{centroid}}} I(f_{\text{LOCO}}(x_i) = r_j)}{|\mathcal{X}_{\text{centroid}}|}$$

end for

end for

Soft misclassification As an alternative to using the final prediction results to compute the *indistinguishability* score, we could instead take a step back by considering the entire distribution from the last activation function, which computes a probability for each possible realization in the output set \mathcal{Y} . In the soft classification setting, we could have the classifier output the entire multinomial distribution, consider the Softmax activation function as an example, $\{\text{softmax}_f(y|x_i)\}_{y \in \mathcal{Y}}$ as opposed to just the label with the maximum score $y^* := \max_y \{P_f(y|x_i)\}_{y \in \mathcal{Y}}$. Therefore the misclassification distribution for computing *indistinguishability* could also be computed as:

$$P_f(\mathcal{X}_{r_i}, r_i, r_j) = \frac{\sum_{x \in \mathcal{X}_{r_i}} \text{softmax}_f(r_j|x)}{|\mathcal{X}_{r_i}|} \quad (4)$$

Aggregated Indistinguishability The *aggregated indistinguishability* for a region r_i is defined as the sum of the pairwise indistinguishability between r_i and all other regions $r_j \neq r_i$:

$$\text{Aggregated Indistinguishability}(r_i) = \sum_{j \neq i} \text{Indistinguishability}(\mathcal{X}_{r_i}, \mathcal{X}_{r_j}),$$

Substituting the definition for pairwise indistinguishability, the aggregated indistinguishability becomes:

$$\text{Aggregated Indistinguishability}(r_i) = \sum_{j \neq i} [P_f(\mathcal{X}_{r_i}, r_i, r_j) + P_f(\mathcal{X}_{r_j}, r_j, r_i)]. \quad (5)$$

Connection to TPV and PPV The True Positive Value (TPV) and Positive Predictive Value (PPV) for region r_i could be written as:

$$\begin{aligned} \text{TPV}_{r_i} &= 1 - \sum_{j \neq i} P_f(\mathcal{X}_{r_i}, r_i, r_j), \\ \text{PPV}_{r_i} &= 1 - \sum_{j \neq i} P_f(\mathcal{X}_{r_j}, r_j, r_i). \end{aligned}$$

Thus, the aggregated indistinguishability for region r_i is equivalently given by:

$$\text{Aggregated Indistinguishability}(r_i) = 2 - (\text{TPV}_{r_i} + \text{PPV}_{r_i}). \quad (6)$$

3 Experiments and Results

3.1 Data and preprocessing

Data For our study, we used a dataset of 551,230 SARS-CoV-2 genome sequences with a maximum length 34,692 from 198 regions. The genome data recorded the SARS-CoV-2 genome sequences along with the location where and the date when they were discovered. Data were obtained from the GISAID database and used as per the GISAID Terms of Use. For a list of genomes, acknowledgement of Originating and/or Submitting Laboratory please see Supplemental Table 4.

Preprocessing This dataset presents two major challenges that affect its analysis: data imbalance and computation complexity brought by the length of the genome sequences. Specifically, the data availability is significantly more ample in the UK, the US and Italy than the rest of the world and it also include minority classes with very few datapoints to learn their patterns. Secondly, the average whole genome sequence length is over 30,000 and the lack of pre-trained base-model for whole genome sequence data makes training of the deep learning neural network computationally expensive and prone to overfit.

To address these challenges, for our experiments, an equal number of genomes are sampled from countries whose data availability passed a certain threshold, resulting in a dataset with equal regional representation. The smaller this threshold, the larger the output set for the MCC problem. The sampling threshold and the sample size from each region, determines the data size and hence computational complexity of solving the classification problem. Hence, the exact architecture used for the classification problem varies with the experiment setting, which in turn determines the computation complexity of the problem.

Further, to investigate the evolutionary timeline of the SARS-CoV-2 genomes, such as identifying the point of evolutionary divergence, our experiment involved a temporal analysis that considered genome association variation at varying timepoints to understand how the virus has evolved over time, enabling us to trace back to the periods of significant genetic shifts and to assess the pace of the evolution.

Baseline: kmers for Naive Bayes classification We chose Kmer pre-processing coupled with Naive Bayes as a baseline approach for GMNA since its computation cost is independent of the length of the sequences. For kmer-based Naïve Bayes modelling, the genome sequences were first transformed into sequences of Kmer words of which the letters are the nucleotides. The K-mer words pre-processing could be considered as using a sliding window of size k to scan through the genome sequences of size L to obtain a sequence of size $L-k+1$ composed of words of length k . The Naive Bayes model assumes Bayes' theorem and conditional feature independence, in this case the Kmer genome subsequence frequencies are assumed to be conditionally independent given the region class labels.

Padding and one-hot encoding for DNN We determined the length of the longest sequence in the genome set and padded all sequences to this maximum length. The padded sequences are then one-hot encoded to obtain a numerical representation of the genome sequences that could be fed to a neural network. After this transformation, the data is represented by a tensor of shape $\text{max length} \times (\text{number of distinctive bases} + 1) \times \text{number of genome sequences}$.

3.2 Evaluation

The performance of the framework could be assessed from four aspects:

Qualitative comparison with the ground truth The alignment between the implications from the misclassification network and expected outcome based on reality or prior knowledge could also be used to validate the efficacy of the MNA framework. For example, in this work, we are expecting the genomes to exhibit spatial dependencies based on the assumption that traveling and social contacts have a significant impact on the *indistinguishability* between genome ensembles. By considering the process of disease spreading and hence genome replications as a random walk, we hypothesize that the degrees of separation between genomes is positively correlated to the probability of mutations during RNA replications. To define the degrees of separation in this context, if a person A contracted the disease from B and similarly B from C, then the genome from A is one degree from the genome from B and 2 degrees away from the genome from the person C. Meanwhile, we assume the degrees of separation among hosts and hence genomes are inversely related to their geographical proximity. Thereby, we expect genomes found in neighboring regions to exhibit stronger associations and hence greater *indistinguishability*.

Classification performance The classification performance, e.g., prediction accuracy, of the trained machine could be considered as an indicator of the intelligence of the machine. The more intelligent the machine, the more credible the suggested association is between the incorrectly predicted class and the true class.

Robustness to the choice of models and classifier accuracy The robustness of the results could be assessed by comparing the misclassified instances produced by different machine learning models and their sensitivity to the classifier accuracy. The inferences obtained from the misclassification network should be resistant to changes in the ML model used for classification. On the other hand, if the misclassification network produced by a weak classifier is consistent with that produced by a strong classifier, the results are considered to be more stable.

Comparison with its configuration network The significance of the results could be assessed by comparing the obtained misclassification network with its configuration network that preserves the same weighted degree sequence, but permuting the connections within the network. This means that the regions they got misclassified as are shuffled while keeping the misclassification probability of each region constant. The configuration model could be used as a null model to analyze whether the identified patterns in the true misclassification network could also be found in its configuration network where all network structures except for the connections between nodes are randomized and perturbed. This comparison helps to determine whether the observed patterns are merely a result of the indistinguishability of each genome ensemble.

3.3 Results

3.3.1 Spatial Analysis: SARS-CoV-2 genomes exhibit strong spatial dependencies

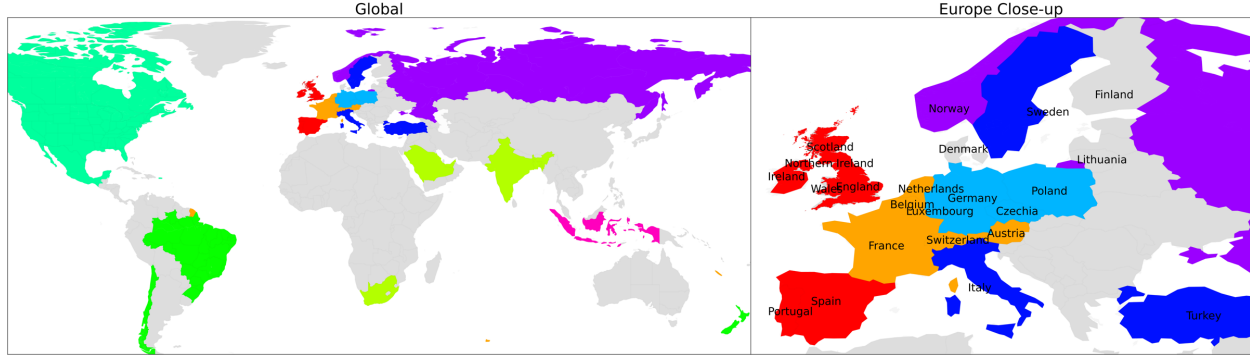
Our results demonstrate the strong spatial dependencies in SARS-CoV-2 genomes, as shown by the community detection results on the misclassification network. Firstly, we demonstrate the applicability of our proposed framework MNA under the multiclass setting 2.1.1. We sampled 300 sequences from each region to ensure broad representation and inclusion of most regions in the analysis. To build the misclassification network, classifiers are trained to predict the origin of genome sequences as outlined in Sec. 2. The pairwise relations between the true and predicted classes are aggregated to construct the misclassification network, which is then partitioned by the Louvain community detection algorithm. The resulting communities, visualized in Fig. 2a, reveal that regions with close geographic proximity around the globe are often partitioned into the same community by the community detection algorithm, which means that the genome sequences from neighboring regions are more indistinguishable from each other. These results support our hypothesis that misclassified instances capture meaningful correlations and could be utilized for inference. Genomes from geographically close regions are more indistinguishable, supporting the assumption that travel and social interactions contribute to genome similarity.

In the true misclassification network in Fig. 2a, Ireland and the UK's four constituent countries along with Spain and Portugal form a distinct community. Other neighboring regions grouped together include: Canada, the United States and Mexico in North America; Brazil and Chile in South America; Germany, Czech Republic, Poland, Luxembourg in Central Europe; Belgium, Denmark, France, the Netherlands, and Austria in Northwestern Europe; Saudi Arabia, United Arab Emirates, India, Bangladesh, and South Africa in the Middle East, South Asia, and Southern Africa; and Indonesia and Singapore in Southeast Asia. Additionally, we provide a network visualization of the GMNA results in Fig.3.

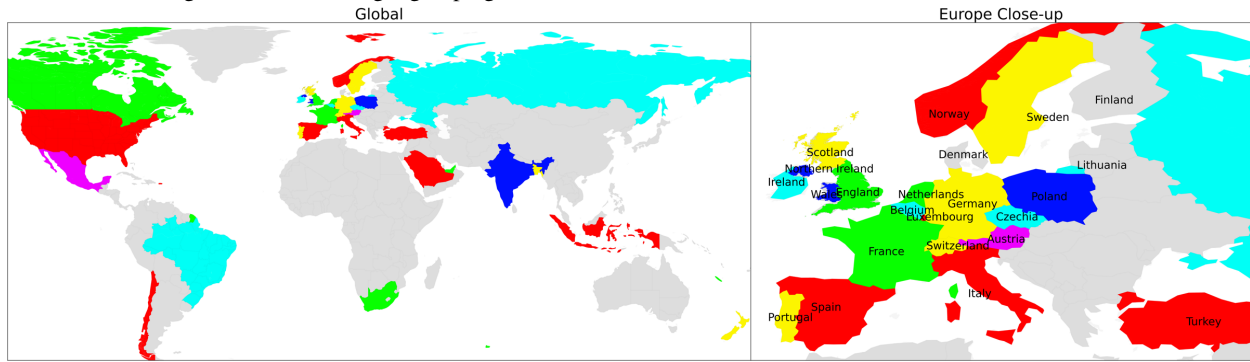
The configuration model provides a null hypothesis by preserving regional genome indistinguishability scores but permuting the connections. Comparing the observed misclassification network with the configuration model (Fig. 2b) allows us to assess whether the observed spatial dependency patterns are significant or merely artifacts.

Secondly, we demonstrate MNA under the binary setting (see 2.1.1), using selected centroid countries from different continents. As described in 2.1.1, the resulting misclassification network from the binary classification setting is a star network, with edges connecting the centroid country to the rest of the world. The edge weights represent the indistinguishability between the centroid and the other regions, computed by training a binary classifier on genome sequences from the centroid region and each of the other regions, and then calculating an indistinguishability score based on the misclassification results.

We visualize the results using different centroid countries, with the redness of the regions indicating their indistinguishability to the centroid region. As shown in Fig. 4, for each selected centroid country, our results indicate that the majority of misclassifications occur between the centroid country and its neighboring countries. In North America, for example, genome sequences from the United States are most frequently misclassified as being from Canada and Mexico. In Asia, genomes from India are most frequently misclassified as those from Bangladesh and the UAE. In Europe, genome sequences from France are mostly misclassified as those from other neighboring European countries, such



(a) Genome Misclassification Results Under the Multiclass Setting: Regions are colored based on Louvain community detection applied to the misclassification network, where the same color represents regions within the same community. A Naive Bayes multiclass model was used with a sample size and threshold of 300. Singular communities (one region) are annotated but left uncolored to distinguish them from larger groupings.



(b) The configuration network of the The community partition of the configuration model is shown, where the degree (indistinguishability score) of each region is preserved, but the connections are randomized to assess the significance of the spatial dependencies observed in (a).

Figure 2: MCC Misclassification vs. Configuration Clustered by the Louvain Community Detection Algorithm: Our results show the SARS-CoV-2 genomes exhibit strong spatial dependencies. Genomes from neighboring regions are highly indistinguishable, and the significance of the findings is supported by the configuration model test.

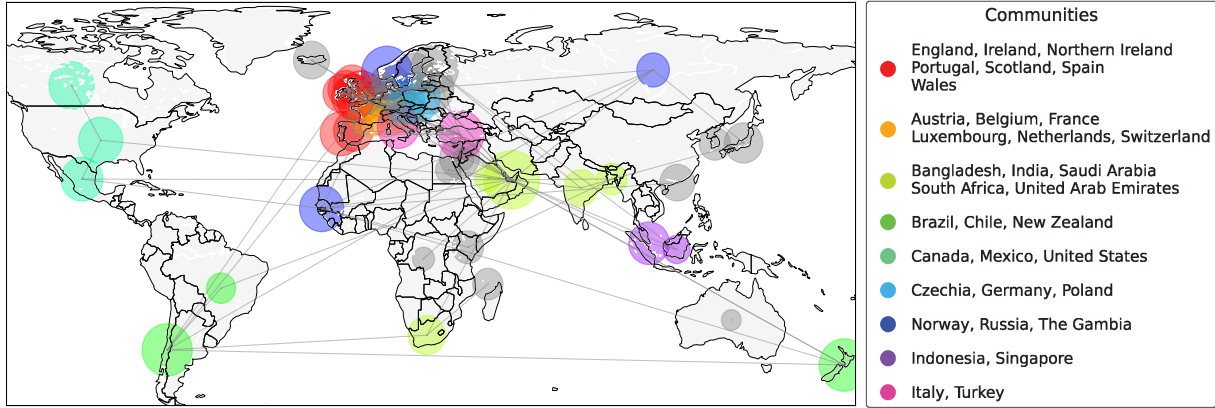


Figure 3: Network Visualization of Misclassification Results in Fig. 2a: In this genome misclassification network, each node represents a subset of genome sequences from a specific region, with edge weights representing the indistinguishability score, computed as the symmetrised empirical likelihood of misclassification between genomes from the two regions. The partition and coloring of the regions are based on community detection clustering results, with singular communities consisting of only one region colored in grey. This plot shows the top 20% edges with the greatest weights.

as Switzerland, Belgium, Luxembourg, and England. When France and England are used as the centroid countries, almost no misclassification occurs outside of Europe. For the UK, genomes from England are mostly misclassified with those from Northern Ireland, Wales, Scotland, Ireland, and France. Notably, Greenland is colored based on the results from Denmark, as it is considered Danish territory, and no experiments were conducted specifically using data from Greenland.

3.4 True Misclassification vs. Configuration

To further validate the significance of the spatial dependencies observed in the binary Naive Bayes (NB) misclassification network, we compared the true misclassification network with its corresponding configuration model in Fig. 5b, similar to the comparison already shown for the multiclass setting in Fig. 2b. Similarly, we observe that communities identified in the configuration graph show no spatial dependency. In Fig. 2b, under the multiclass setting, the neighboring regions are often from different communities. And in the binary true misclassification network in Fig. 5a, with England as the centroid, again, we observe that most of England genomes that got misclassified are distributed around its neighboring regions, most frequently, Scotland, Wale, Ireland and France. In general, the misclassified instances happened most frequently to the European regions and least frequently to North America and Asia. In the configuration graph, the most frequently misidentified regions are randomly scattered around the map as opposed to being close to the region of interest, England.

3.5 Impact of International Travel on COVID Genome Variation

We investigated the impact of international travel activities on the evolution and variation of COVID genomes, by assessing the country-level aggregated indistinguishability of COVID sequences from both spatial and temporal perspectives. We quantified these impacts by examining the correlation between the centrality of countries in the OAG flight network and their respective country-level aggregated genome indistinguishability computed by misclassification rates. Our findings in Table 2 show significant correlations between travel activities and the aggregated pairwise genome sequence indistinguishability. The regional travel acitivities were assessed by their degree, eigenvector, closeness, and betweenness centralities within the flight network. The identified correlations suggest that countries with more central roles in international travel exhibit more complex COVID genome compositions, reflecting the influence of travel on genomic variations. Additionally, these results align well with the assumptions underlying the proposed GMNA framework, that travel and social contacts likely enhance homogeneity among epidemic genome ensembles from neighboring regions. This assumption could explain why genomes from more international regions exhibit higher aggregated indistinguishability. These results show the importance of taking the underlying transportation network into account when understanding and responding to the genomic evolution of COVID-19 and other epidemics. Further, using genomes from different time points, we examined the association between the emergence of Variants of Concern (VOCs) and the average aggregated genome indistinguishability scores, as depicted in Fig. 7. Our results show that the accuracy of genome region prediction steadily increased at the beginning of COVID from around 0.84 in April 2020 to 0.96 in August 2020, suggesting developments of stronger regional characteristics during this period. The declined accuracy and hence increased aggregated genome indistinguishability after the emergence of Alpha, Delta, and Gamma variants could potentially be explained by variants mixing resulted by international travel.

Centrality Measure	Spearman's Rank Correlation Coefficients	P-value
Degree	0.550	2.55e-06
Eigenvector	0.584	4.12e-07
Closeness	0.554	2.05e-06
Betweenness	0.378	2.05e-03

Table 2: Correlation between Centralities in the Flight Network and COVID Genome Sequence Indistinguishability: The identified correlations show that countries with more central roles in international travel have more complex COVID genome compositions, highlighting the effect of travel on genomic variations.

3.6 Classification Accuracy

In machine learning, improving performance of a trained classifier often serves as the primary research goal. While higher accuracy generally indicates a more reliable and credible model, it also results in limited data availability for misclassification-based inference. Consequently, a higher-accuracy classifier may not be the optimal option when the research objective is to learn from the misclassified instances.

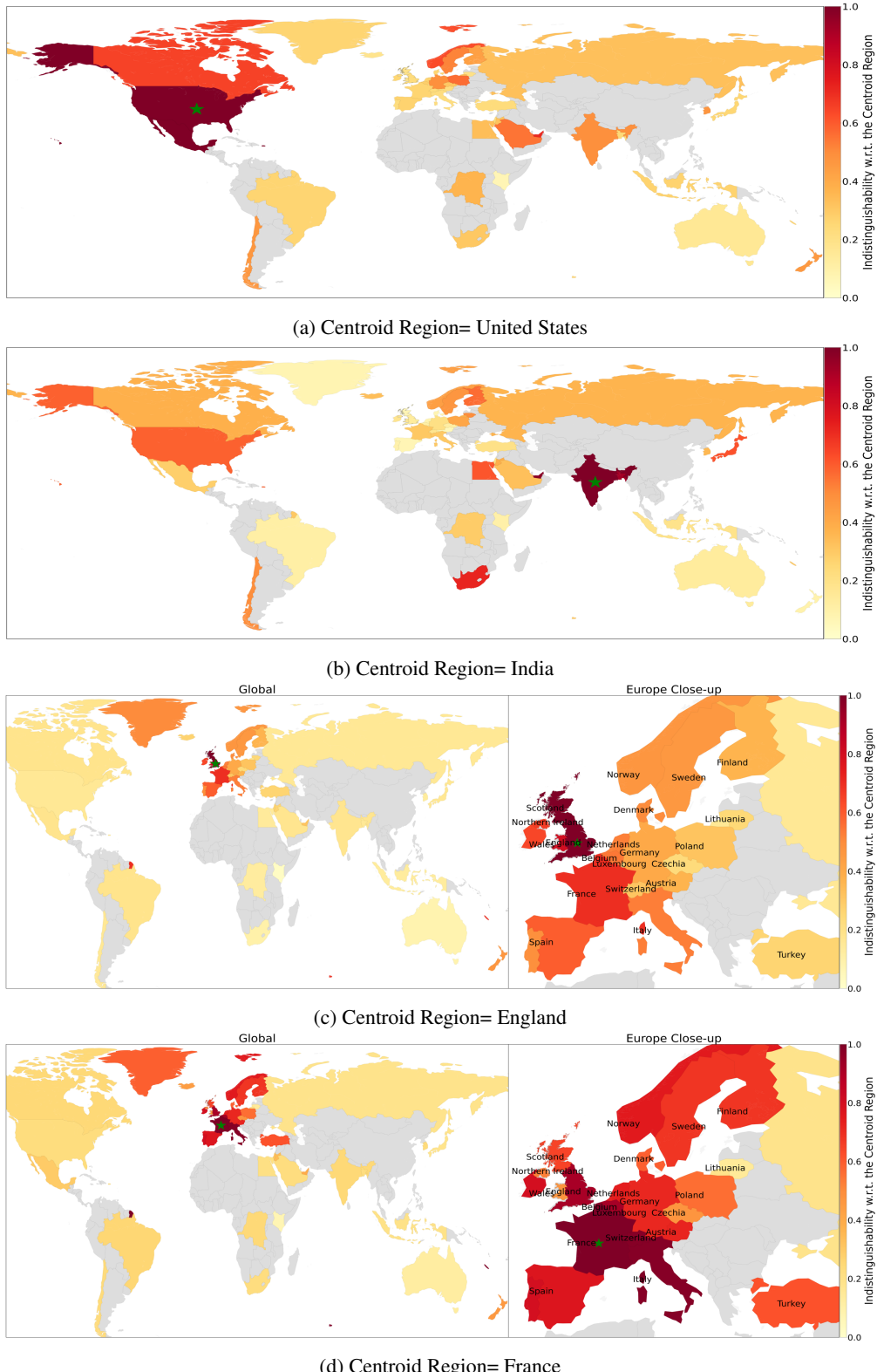


Figure 4: Binary Naive Bayes Misclassification: The spatial dependencies among COVID genomes are also evident under the binary classification setting. Each subplot corresponds to a different centroid country, and a star misclassification network is constructed based on the Naive Bayes binary classification results relative to the centroid country. In (c) and (d), we are also showing the Europe close-ups of the misclassification networks on the right.

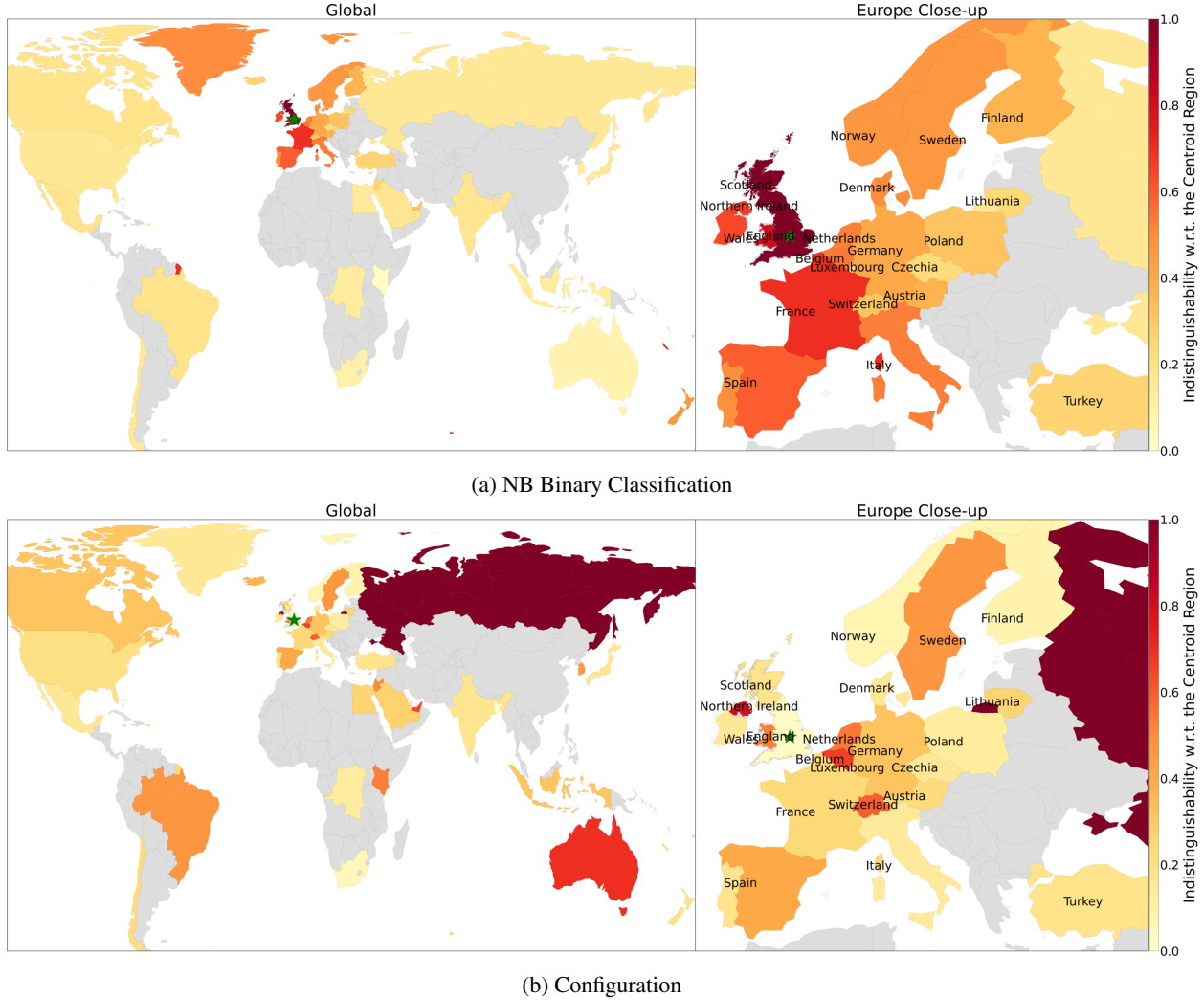


Figure 5: Binary NB Misclassification Network vs. Configuration: The significance of the spatial dependencies is supported by the configuration model test. The misclassification network constructed under the binary scheme is a star network, relative to the centroid England. The redness of the other regions are determined by its indistinguishability score with respect to genomes from England.

For example, under the binary setting, a CNN classifier could easily achieve close to 100% classification accuracy. Although the misclassified instances produced by a higher-performance classifier intuitively suggest stronger class-wise associations, an overly accurate binary classifier that generates few misclassified instances offers limited insights into the genome associations. Moreover, the LOCO algorithm (see Section 2.1.1) we designed to handle the trade-off between classification accuracy and the availability of misclassified data can only be applied to the multiclass classification setting, not the binary setting. Hence, for all experiments conducted under the binary setting, we use the Naive Bayes classifier to allow for more misclassified instances.

Similarly, under the multiclass classification setting, though from the perspective of model performance, deep learning-based models could classify genome sequences with higher accuracy, the results may be less informative for misclassification-based inference. This is because they require more data to train, resulting in datasets with reduced regional representation. Additionally, higher accuracy may result in outcomes with minimal gradient, with misclassified instances predominantly occurring in overt situations. As shown in Fig. 9b, though the misclassification network from a more accurate CNN classifier still displays spatial dependency, the less inclusive dataset yields results that are comparatively less informative or comprehensive compared to Fig. 5a. Hence, we emphasize that the main purpose of this project is not to push the classification accuracy of the employed classifier, but to show the applicability of using the misclassified instances for association inference.

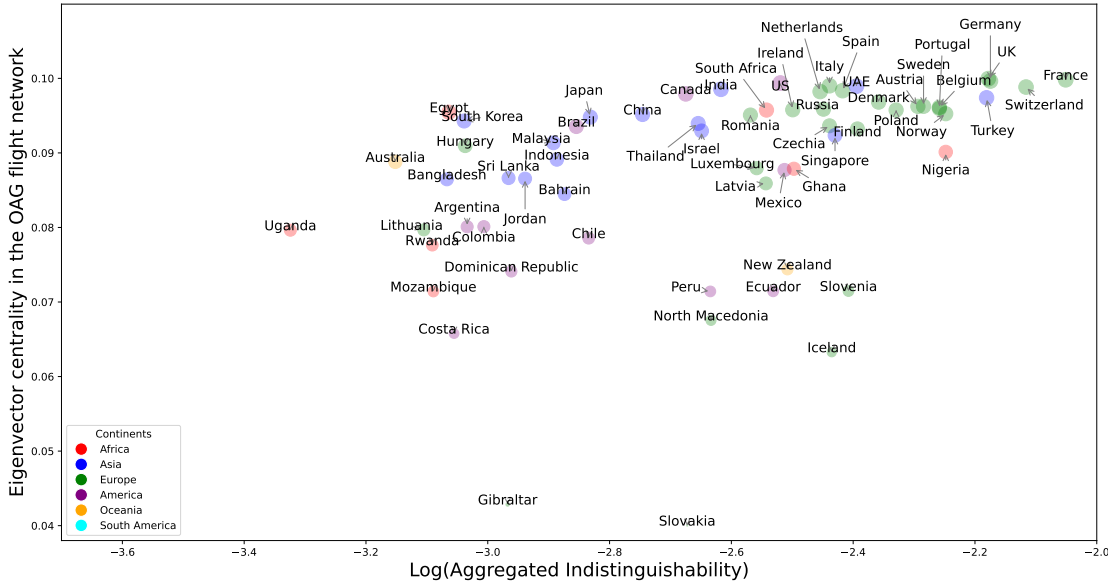


Figure 6: Eigenvector Centrality vs. Log-Transformed Aggregated Indistinguishability of COVID Genome Sequences by Country: Countries are color-coded by continent. Countries with greater travel connectivity, particularly in Europe and Asia, tend to exhibit higher genome sequence indistinguishability.

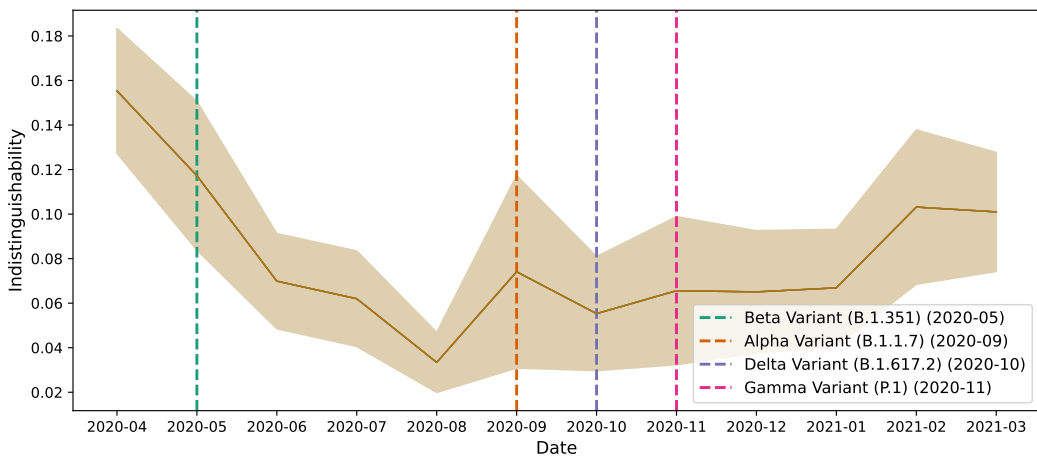


Figure 7: Genome Indistinguishability with respect to Time and COVID VOC Occurrences: The figure shows the temporal relationship between genome indistinguishability and the emergence of Variants of Concern (VOCs). The indistinguishability of genome regions started at around 0.16 in April 2020 and declined steadily to 0.04 by August 2020, indicating the development of stronger regional genome characteristics. However, after the emergence of VOCs such as Alpha, Delta, and Gamma, the indistinguishability increased with fluctuation, suggesting increased genome variation, potentially due to the mixing of variants driven by international travel. The shaded area represents the 95% confidence interval of the accuracy score.

We provide examples of model performance for reference in Table 3. As described in 3.1, we sample an equal number of genomes from countries whose data availability surpasses a certain threshold, resulting in a dataset with equal regional representation. The threshold value determines the number of regions for prediction. The sample size from each region and the size of the label set, representing the number of classes for the classification problem, directly impact the data size, computational complexity, and model performance.

Model Name	Accuracy	Threshold	Sample Size	Label Set Size
Binary CNN	99.0%	1000	1000	33
Binary Naive Bayes (centroid=England)	89.5%	100	100	33
Binary Naive Bayes (centroid=France)	88.3%	100	100	33
Binary Naive Bayes (centroid=United States)	92.5%	100	100	33
Binary Naive Bayes (centroid=India)	95.6%	100	100	33
Multiclass CNN	86.5%	10000	10000	9
Multiclass CNN	75.6%	3000	3000	20
Multiclass CNN	60.9%	1000	1000	33
Multiclass Naive Bayes	64.9%	300	300	49
Enformer+CNN fine tune	68.9%	10000	10000	9

Table 3: Model Performance under Different Settings. The table shows the accuracy of the models used in this study for reference. While higher accuracy is often a goal in machine learning, this study emphasizes that overly accurate classifiers may reduce the utility of misclassified instances for association inference. Classifiers with higher accuracy, such as CNNs, produce minimal misclassification, leading to association results with limited gradient and reduced detail. The results shown here highlight that the aim of our framework is not to maximize accuracy, but to use misclassification as a tool for exploring complex genomic relationships.

4 Discussion

In this work, we present a novel alignment-free approach for comparative genomics that we term the genome misclassification network analysis (GMNA). Our framework is a generic network-generating method based on misclassification results for correlation-based network analysis. We introduce *indistinguishability*, to quantify the association between pairs of genome groups and the genetic diversity of genome ensembles. We identify the pairwise association between the target outcome and the predicted outcome, which is then utilized to design a data-driven framework that can incorporate any state-of-the-art AI models for comparative genome analysis. We showed using more than 500,000 SARS-CoV-2 genomes that by employing GMNA, associations between sequences and geographic sampling location could be uncovered with limited computation resources.

Using our framework GMNA, we showed that SARS-CoV-2 genome sequences exhibit strong geographic clustering and the results are robust and consistent under various experimental settings. Further, the genome ensemble indistinguishabilities, which could indicate genetic variation and complexity, could be correlated to the centralities of their positions in a travel network, i.e. the OAG flight network. The centrality of a region in the flight network indicates its importance in global transportation. And this result suggests that human activities impact COVID genome variation. Additionally, we considered how the average indistinguishability of the genome sequences evolve during COVID and compared it with the emergence of the variants of concerns.

Previous efforts to classify SARS-CoV-2 genomes have focused on lineages tracking and identification using established comparative phylogenetic approaches [37, 87, 98, 114] and those based on k-mer clustering [5, 4, 105] have overall found high accuracy. Additionally, there have been some efforts leveraging neural networks to predict SARS-CoV-2 infection [15, 91, 109] or detect SARS-CoV-2 from different virus strains [60, 67, 75], which—in agreement with our findings—demonstrate the utility of such ML-based methodologies. These studies contribute to a growing body of literature on the utility of ML/AI models in studying emerging infectious disease outbreaks [8, 45, 92, 11, 68]. Our results extend from these approaches by highlighting the information contained in the misclassification network, which is relevant for both comparative and ML-based models. Future work should focus on linking comparative and ML approaches as a way of improving the explainability of the ML-models and investigating whether different ML approaches have favorable properties with respect to data training efficiency and/or generalizability.

Our results demonstrating an association between travel and SARS-CoV-2 genome misclassification is not unexpected. Indeed, we see this results as validating our underlying modeling approaches. Previous phylogeographic studies of SARS-CoV-2 have found strong impacts of mobility on genome differentiation [57, 32, 66, 41]. Coupled with studies of the effect of mobility on the underlying epidemiology of SARS-CoV-2 [58, 28, 106, 90, 24], our findings

contribute to a growing body of evidence showing the strong dependence of epidemic dynamics on mobility [25, 107, 9]. This finding, that mobility structures pathogen genomes and epidemic dynamics, has been found across a range of established [25, 64, 82], emerging [113, 2, 56, 58, 28, 106, 90, 24, 81], and re-surging [107, 48] pathogens across a range of transmission routes and pathogen type, e.g., bacterial vs. viral. Again, that host mobility leaves a detectable signature on pathogen genomics has been well studied both theoretically [94, 19, 23, 86] and empirically [61, 85, 25] and is thought to be a quite general feature of population genetic differentiation [83, 65, 63, 108, 36].

Regarding the choice of model for classification, our results show that Naive Bayes performed sufficiently well for genome comparative analysis. We include results incorporating a CNN-based model in the GMNA framework that demonstrate similar spatial dependency in the appendix 8a. Additionally, we employed a transfer learning approach by fine-tuning a pre-trained transformer-based [101] model, specifically the Enformer [13], for our genome classification task. However, contrary to our expectations, we did not observe an improvement in performance compared to the CNN model for this task. The classification performance from fine-tuning the Enformer is included in Table 3 for reference. We note that methods incorporating prior knowledge, such as negative sampling [70, 69], have been shown to improve model performance by taking into account both similarity and dissimilarity in data context. However, we chose not to employ such techniques in our study, since the purpose of our study is to learn data associations, which would have been compromised if assumptions about data association were already incorporated during model training.

One additional limitation of this data association computation framework is that it only considers the association between groups of data and does not compare singular data points. However, we do not attempt to measure the association between two singular genomes or correlate such singular associations to their features, for the reason that the results would be lack of statistical significance. Indeed, the measured correlations and inferred associations between observable traits of individual sequences may not be reliably representative or comprehensive.

Overall, our study demonstrates the effectiveness of GMNA in identifying valuable information from misclassification data and providing insights into the spatial dependencies and potential factors contributing to the variation in SARS-CoV-2 genomes. Notably, misclassified instances during AI model training are often overlooked during results interpretation. Our proposed framework allows for the recycling of these misclassified instances, and our results show that misclassifications in genome sequencing data could provide insights into genetic variations associated with travel. We believe that repurposing misclassified instances holds promise in a wide range of applications beyond the scope of our study, such as healthcare, medical imaging, and diagnosis.

Code and Data Availability

The code supporting the findings of this research is available in the GitHub repository, accessible at <https://github.com/wanhe13/Genome-Misclassification-Network-Analysis-GMNA->. The repository includes all non-genomic data (see below for accessing those data), scripts, and instructions necessary to replicate the analyses presented in this study.

GISAID Identifier:	EPI_SET_20220727na
DOI:	10.55876/gis8.220727na

Table 4: **Data availability and Acknowledgements** - All genome sequences and associated metadata in this dataset are published in GISAID's EpiCoV database. Anyone with valid GISAID Access Credentials can retrieve all records encompassed in the EPI_SET ID. Those without GISAID Access Credentials may retrieve information about all contributors of data on which our analysis is based by either clicking on the DOI, or pasting the EPI_SET ID in the "Data Acknowledgement Locator" on the GISAID homepage. To view the contributors of each individual sequence with details such as accession number, Virus name, Collection date, Originating Lab and Submitting Lab and the list of Authors, visit: 10.55876/gis8.220727na.

The reported Enformer+CNN model used the pretrained Enformer weights from <https://huggingface.co/EleutherAI/enformer-official-rough>.

Acknowledgements

We would like to thank Professor Mortiz UG Kraemer for assistance acquiring and curating the genomic data and conversations about earlier iterations of this work.

References

- [1] Tarik Alafif, Abdul Muneeim Tehame, Saleh Bajaba, Ahmed Barnawi, and Saad Zia. Machine and deep learning towards covid-19 diagnosis and treatment: survey, challenges, and future directions. *International journal of environmental research and public health*, 18(3):1117, 2021.
- [2] Kathleen A Alexander, Claire E Sanderson, Madav Marathe, Bryan L Lewis, Caitlin M Rivers, Jeffrey Shaman, John M Drake, Eric Lofgren, Virginia M Dato, Marisa C Eisenberg, et al. What factors might have led to the emergence of ebola in west africa? *PLoS neglected tropical diseases*, 9(6):e0003652, 2015.
- [3] Jessica Alföldi and Kerstin Lindblad-Toh. Comparative genomics as a tool to understand evolution and disease. *Genome research*, 23(7):1063–1068, 2013.
- [4] Sarwan Ali, Tamkanat E Ali, Muhammad Asad Khan, Imdadullah Khan, and Murray Patterson. Effective and scalable clustering of sars-cov-2 sequences. In *Proceedings of the 5th international conference on big data research*, pages 42–49, 2021.
- [5] Sarwan Ali, Bikram Sahoo, Naimat Ullah, Alexander Zelikovskiy, Murray Patterson, and Imdadullah Khan. A k-mer based approach for sars-cov-2 variant identification. In *Bioinformatics Research and Applications: 17th International Symposium, ISBRA 2021, Shenzhen, China, November 26–28, 2021, Proceedings 17*, pages 153–164. Springer, 2021.
- [6] Stephen F Altschul, Thomas L Madden, Alejandro A Schäffer, Jinghui Zhang, Zheng Zhang, Webb Miller, and David J Lipman. Gapped blast and psi-blast: a new generation of protein database search programs. *Nucleic acids research*, 25(17):3389–3402, 1997.
- [7] Samuel V Angiuoli and Steven L Salzberg. Mugsy: fast multiple alignment of closely related whole genomes. *Bioinformatics*, 27(3):334–342, 2011.
- [8] Sina F Ardabili, Amir Mosavi, Pedram Ghamisi, Filip Ferdinand, Annamaria R Varkonyi-Koczy, Uwe Reuter, Timon Rabczuk, and Peter M Atkinson. Covid-19 outbreak prediction with machine learning. *Algorithms*, 13(10):249, 2020.
- [9] Alex Arenas, Wesley Cota, Jesús Gómez-Gardeñes, Sergio Gómez, Clara Granell, Joan T Matamalas, David Soriano-Paños, and Benjamin Steinegger. Modeling the spatiotemporal epidemic spreading of covid-19 and the impact of mobility and social distancing interventions. *Physical Review X*, 10(4):041055, 2020.
- [10] Joel Armstrong, Ian T Fiddes, Mark Diekhans, and Benedict Paten. Whole-genome alignment and comparative annotation. *Annual review of animal biosciences*, 7(1):41–64, 2019.
- [11] Gunjan Arora, Jayadev Joshi, Rahul Shubhra Mandal, Nitisha Shrivastava, Richa Virmani, and Tavpritesh Sethi. Artificial intelligence in surveillance, diagnosis, drug discovery and vaccine development against covid-19. *Pathogens*, 10(8):1048, 2021.
- [12] Ehsaneddin Asgari, Kiavash Garakani, Alice C McHardy, and Mohammad RK Mofrad. Micropheno: predicting environments and host phenotypes from 16s rrna gene sequencing using a k-mer based representation of shallow sub-samples. *Bioinformatics*, 34(13):i32–i42, 2018.
- [13] Žiga Avsec, Vikram Agarwal, Daniel Visentin, Joseph R Ledsam, Agnieszka Grabska-Barwinska, Kyle R Taylor, Yannis Assael, John Jumper, Pushmeet Kohli, and David R Kelley. Effective gene expression prediction from sequence by integrating long-range interactions. *Nature methods*, 18(10):1196–1203, 2021.
- [14] Shakuntala Baichoo and Christos A Ouzounis. Computational complexity of algorithms for sequence comparison, short-read assembly and genome alignment. *Biosystems*, 156:72–85, 2017.
- [15] Abhirup Banerjee, Surajit Ray, Bart Vorselaars, Joanne Kitson, Michail Mamalakis, Simonne Weeks, Mark Baker, and Louise S Mackenzie. Use of machine learning and artificial intelligence to predict sars-cov-2 infection from full blood counts in a population. *International immunopharmacology*, 86:106705, 2020.
- [16] Ziv Bar-Yossef, TS Jayram, Robert Krauthgamer, and Ravi Kumar. Approximating edit distance efficiently. In *45th Annual IEEE Symposium on Foundations of Computer Science*, pages 550–559. IEEE, 2004.
- [17] Bo Ram Beck, Bonggun Shin, Yoonjung Choi, Sungsoo Park, and Keunsoo Kang. Predicting commercially available antiviral drugs that may act on the novel coronavirus (sars-cov-2) through a drug-target interaction deep learning model. *Computational and structural biotechnology journal*, 18:784–790, 2020.
- [18] B Edwin Blaisdell. A measure of the similarity of sets of sequences not requiring sequence alignment. *Proceedings of the National Academy of Sciences*, 83(14):5155–5159, 1986.
- [19] Michael Boots and Michael Mealor. Local interactions select for lower pathogen infectivity. *Science*, 315(5816):1284–1286, 2007.

[20] David G Brown and Frank W Samuelson. Pitfalls and opportunities in the development and evaluation of artificial intelligence systems. In *Artificial Intelligence in the Age of Neural Networks and Brain Computing*, pages 173–192. Elsevier, 2024.

[21] Roberto Cahuantzi, Katrina A Lythgoe, Ian Hall, Lorenzo Pellis, and Thomas House. Unsupervised identification of significant lineages of sars-cov-2 through scalable machine learning methods. *Proceedings of the National Academy of Sciences*, 121(12):e2317284121, 2024.

[22] Constantine Caramanis, Dimitris Fotakis, Alkis Kalavasis, Vasilis Kontonis, and Christos Tzamos. Optimizing solution-samplers for combinatorial problems: The landscape of policy-gradient method. *Advances in Neural Information Processing Systems*, 36:14035–14069, 2023.

[23] Carlos Castillo-Chavez, Derdei Bichara, and Benjamin R Morin. Perspectives on the role of mobility, behavior, and time scales in the spread of diseases. *Proceedings of the National Academy of Sciences*, 113(51):14582–14588, 2016.

[24] Meng-Chun Chang, Rebecca Kahn, Yu-An Li, Cheng-Sheng Lee, Caroline O Buckee, and Hsiao-Han Chang. Variation in human mobility and its impact on the risk of future covid-19 outbreaks in taiwan. *BMC public health*, 21:1–10, 2021.

[25] Vivek Charu, Scott Zeger, Julia Gog, Ottar N Bjørnstad, Stephen Kissler, Lone Simonsen, Bryan T Grenfell, and Cécile Viboud. Human mobility and the spatial transmission of influenza in the united states. *PLoS computational biology*, 13(2):e1005382, 2017.

[26] Ayan Chatterjee, Robin Walters, Zohair Shafi, Omair Shafi Ahmed, Michael Sebek, Deisy Gysi, Rose Yu, Tina Eliassi-Rad, Albert-László Barabási, and Giulia Menichetti. Improving the generalizability of protein-ligand binding predictions with ai-bind. *Nature communications*, 14(1):1989, 2023.

[27] Rajashree Chaurasia and Udayan Ghose. Human dna/rna motif mining using deep-learning methods: a scoping review. *Network Modeling Analysis in Health Informatics and Bioinformatics*, 12(1):20, 2023.

[28] Matteo Chinazzi, Jessica T Davis, Marco Ajelli, Corrado Gioannini, Maria Litvinova, Stefano Merler, Ana Pastore y Piontti, Kunpeng Mu, Luca Rossi, Kaiyuan Sun, et al. The effect of travel restrictions on the spread of the 2019 novel coronavirus (covid-19) outbreak. *Science*, 368(6489):395–400, 2020.

[29] Francesc Coll, Ruth McNerney, Mark D Preston, José Afonso Guerra-Assunção, Andrew Warry, Grant Hill-Cawthorne, Kim Mallard, Mridul Nair, Anabela Miranda, Adriana Alves, et al. Rapid determination of anti-tuberculosis drug resistance from whole-genome sequences. *Genome medicine*, 7:1–10, 2015.

[30] Wouter Deelder, Emilia Manko, Jody E Phelan, Susana Campino, Luigi Palla, and Taane G Clark. Geographical classification of malaria parasites through applying machine learning to whole genome sequence data. *Scientific reports*, 12(1):21150, 2022.

[31] Jacob Devlin, Ming-Wei Chang, Kenton Lee, and Kristina Toutanova. Bert: Pre-training of deep bidirectional transformers for language understanding. *arXiv preprint arXiv:1810.04805*, 2018.

[32] Gytis Dudas, Samuel L Hong, Barney I Potter, Sébastien Calvignac-Spencer, Frédéric S Niatou-Singa, Thais B Tombolomako, Terence Fuh-Neba, Ulrich Vickos, Markus Ulrich, Fabian H Leendertz, et al. Emergence and spread of sars-cov-2 lineage b. 1.620 with variant of concern-like mutations and deletions. *Nature communications*, 12(1):5769, 2021.

[33] Hans Ellegren. Comparative genomics and the study of evolution by natural selection. *Molecular ecology*, 17(21):4586–4596, 2008.

[34] Gökçen Eraslan, Žiga Avsec, Julien Gagneur, and Fabian J Theis. Deep learning: new computational modelling techniques for genomics. *Nature Reviews Genetics*, 20(7):389–403, 2019.

[35] Antonino Fiannaca, Laura La Paglia, Massimo La Rosa, Giosue’ Lo Bosco, Giovanni Renda, Riccardo Rizzo, Salvatore Gaglio, and Alfonso Urso. Deep learning models for bacteria taxonomic classification of metagenomic data. *BMC bioinformatics*, 19:61–76, 2018.

[36] Martin C Fischer, Christian Rellstab, Marianne Leuzinger, Marie Roumet, Felix Gugerli, Kentaro K Shimizu, Rolf Holderegger, and Alex Widmer. Estimating genomic diversity and population differentiation—an empirical comparison of microsatellite and snp variation in arabidopsis halleri. *BMC genomics*, 18:1–15, 2017.

[37] Peter Forster, Lucy Forster, Colin Renfrew, and Michael Forster. Phylogenetic network analysis of sars-cov-2 genomes. *Proceedings of the National Academy of Sciences*, 117(17):9241–9243, 2020.

[38] Santo Fortunato. Community detection in graphs. *Physics reports*, 486(3-5):75–174, 2010.

[39] Kelly A Frazer, Lior Pachter, Alexander Poliakov, Edward M Rubin, and Inna Dubchak. Vista: computational tools for comparative genomics. *Nucleic acids research*, 32(suppl_2):W273–W279, 2004.

[40] Michelle Girvan and Mark EJ Newman. Community structure in social and biological networks. *Proceedings of the national academy of sciences*, 99(12):7821–7826, 2002.

[41] Sama Goliae, Mohammad-Hadi Foroughmand-Araabi, Aideen Roddy, Ariane Weber, Sanni Översti, Denise Kühnert, and Alice C McHardy. Importations of sars-cov-2 lineages decline after nonpharmaceutical interventions in phylogeographic analyses. *Nature Communications*, 15(1):5267, 2024.

[42] Maria Halkidi, Yannis Batistakis, and Michalis Vazirgiannis. On clustering validation techniques. *Journal of intelligent information systems*, 17:107–145, 2001.

[43] Wenkai Han, Ningning Chen, Xinzhou Xu, Adil Sahil, Juexiao Zhou, Zhongxiao Li, Huawei Zhong, Elva Gao, Ruochi Zhang, Yu Wang, et al. Predicting the antigenic evolution of sars-cov-2 with deep learning. *Nature Communications*, 14(1):3478, 2023.

[44] Desmond G Higgins and Paul M Sharp. Clustal: a package for performing multiple sequence alignment on a microcomputer. *Gene*, 73(1):237–244, 1988.

[45] Muhammad Nazrul Islam, Toki Tahmid Inan, Suzzana Rafi, Syeda Sabrina Akter, Iqbal H Sarker, and AKM Nazmul Islam. A systematic review on the use of ai and ml for fighting the covid-19 pandemic. *IEEE Transactions on Artificial Intelligence*, 1(3):258–270, 2020.

[46] Yanrong Ji, Zhihan Zhou, Han Liu, and Ramana V Davuluri. Dnabert: pre-trained bidirectional encoder representations from transformers model for dna-language in genome. *Bioinformatics*, 37(15):2112–2120, 2021.

[47] Wengong Jin, Jonathan M Stokes, Richard T Eastman, Zina Itkin, Alexey V Zakharov, James J Collins, Tommi S Jaakkola, and Regina Barzilay. Deep learning identifies synergistic drug combinations for treating covid-19. *Proceedings of the National Academy of Sciences*, 118(39):e2105070118, 2021.

[48] Ezekiel Kalipeni and Joseph Oppong. The refugee crisis in africa and implications for health and disease: a political ecology approach. *Social science & medicine*, 46(12):1637–1653, 1998.

[49] Michał Karlicki, Stanisław Antonowicz, and Anna Karnkowska. Tiara: deep learning-based classification system for eukaryotic sequences. *Bioinformatics*, 38(2):344–350, 2022.

[50] W James Kent. Blat—the blast-like alignment tool. *Genome research*, 12(4):656–664, 2002.

[51] Daehwan Kim, Joseph M Paggi, Chanhee Park, Christopher Bennett, and Steven L Salzberg. Graph-based genome alignment and genotyping with hisat2 and hisat-genotype. *Nature biotechnology*, 37(8):907–915, 2019.

[52] Gunnar W Klau. A new graph-based method for pairwise global network alignment. *BMC bioinformatics*, 10:1–9, 2009.

[53] Eugene V Koonin, L Aravind, and Alexey S Kondrashov. The impact of comparative genomics on our understanding of evolution. *Cell*, 101(6):573–576, 2000.

[54] Bernhard H Korte, Jens Vygen, B Korte, and J Vygen. *Combinatorial optimization*, volume 1. Springer, 2011.

[55] Joel Kowalewski and Anandasankar Ray. Predicting novel drugs for sars-cov-2 using machine learning from a> 10 million chemical space. *Heliyon*, 6(8), 2020.

[56] Moritz UG Kraemer, Nick Golding, Dionisio Bisanzio, Samir Bhatt, David M Pigott, SE Ray, OJ Brady, JS Brownstein, NR Faria, DAT Cummings, et al. Utilizing general human movement models to predict the spread of emerging infectious diseases in resource poor settings. *Scientific reports*, 9(1):5151, 2019.

[57] Moritz UG Kraemer, Verity Hill, Christopher Ruis, Simon Dellicour, Sumali Bajaj, John T McCrone, Guy Baele, Kris V Parag, Anya Lindström Battle, Bernardo Gutierrez, et al. Spatiotemporal invasion dynamics of sars-cov-2 lineage b. 1.1. 7 emergence. *Science*, 373(6557):889–895, 2021.

[58] Moritz UG Kraemer, Chia-Hung Yang, Bernardo Gutierrez, Chieh-Hsi Wu, Brennan Klein, David M Pigott, Open COVID-19 Data Working Group†, Louis Du Plessis, Nuno R Faria, Ruoran Li, et al. The effect of human mobility and control measures on the covid-19 epidemic in china. *Science*, 368(6490):493–497, 2020.

[59] Xingyan Kuang, Fan Wang, Kyle M Hernandez, Zhenyu Zhang, and Robert L Grossman. Accurate and rapid prediction of tuberculosis drug resistance from genome sequence data using traditional machine learning algorithms and cnn. *Scientific reports*, 12(1):2427, 2022.

[60] Samuel Lalmuanawma, Jamal Hussain, and Lalrinfela Chhakchhuak. Applications of machine learning and artificial intelligence for covid-19 (sars-cov-2) pandemic: A review. *Chaos, Solitons & Fractals*, 139:110059, 2020.

[61] Philippe Lemey, Andrew Rambaut, Trevor Bedford, Nuno Faria, Filip Bielejec, Guy Baele, Colin A Russell, Derek J Smith, Oliver G Pybus, Dirk Brockmann, et al. Unifying viral genetics and human transportation data to predict the global transmission dynamics of human influenza h3n2. *PLoS pathogens*, 10(2):e1003932, 2014.

[62] Jure Leskovec, Kevin J Lang, and Michael Mahoney. Empirical comparison of algorithms for network community detection. In *Proceedings of the 19th international conference on World wide web*, pages 631–640, 2010.

[63] Stephen Leslie, Bruce Winney, Garrett Hellenthal, Dan Davison, Abdelhamid Boumertit, Tammy Day, Katarzyna Hutzik, Ellen C Royston, Barry Cunliffe, Wellcome Trust Case Control Consortium 2, et al. The fine-scale genetic structure of the british population. *Nature*, 519(7543):309–314, 2015.

[64] K Lönnroth, Z Mor, C Erkens, J Bruchfeld, RR Nathavitharana, MJ Van Der Werf, and C Lange. Tuberculosis in migrants in low-incidence countries: epidemiology and intervention entry points. *The International Journal of Tuberculosis and Lung Disease*, 21(6):624–636, 2017.

[65] Liisa Loog, Marta Mirazón Lahr, Mirna Kovacevic, Andrea Manica, Anders Eriksson, and Mark G Thomas. Estimating mobility using sparse data: Application to human genetic variation. *Proceedings of the National Academy of Sciences*, 114(46):12213–12218, 2017.

[66] Mariana G López, Álvaro Chiner-Oms, Darío García de Viedma, Paula Ruiz-Rodríguez, María Alma Bracho, Irving Cancino-Muñoz, Giuseppe D’Auria, Griselda de Marco, Neris García-González, Galo Adrian Goig, et al. The first wave of the covid-19 epidemic in spain was associated with early introductions and fast spread of a dominating genetic variant. *Nature genetics*, 53(10):1405–1414, 2021.

[67] Alejandro Lopez-Rincon, Alberto Tonda, Lucero Mendoza-Maldonado, Daphne GJC Mulders, Richard Molenkamp, Carmina A Perez-Romero, Eric Claassen, Johan Garssen, and Aletta D Kranenveld. Classification and specific primer design for accurate detection of sars-cov-2 using deep learning. *Scientific reports*, 11(1):947, 2021.

[68] Julia L Marcus, Whitney C Sewell, Laura B Balzer, and Douglas S Krakower. Artificial intelligence and machine learning for hiv prevention: emerging approaches to ending the epidemic. *Current HIV/AIDS Reports*, 17:171–179, 2020.

[69] Tomas Mikolov, Kai Chen, Greg Corrado, and Jeffrey Dean. Efficient estimation of word representations in vector space. *arXiv preprint arXiv:1301.3781*, 2013.

[70] Tomas Mikolov, Ilya Sutskever, Kai Chen, Greg S Corrado, and Jeff Dean. Distributed representations of words and phrases and their compositionality. *Advances in neural information processing systems*, 26, 2013.

[71] Webb Miller, Kateryna D Makova, Anton Nekrutenko, and Ross C Hardison. Comparative genomics. *Annu. Rev. Genomics Hum. Genet.*, 5(1):15–56, 2004.

[72] Ilia Minkin and Paul Medvedev. Scalable multiple whole-genome alignment and locally collinear block construction with sibelia. *Nature communications*, 11(1):6327, 2020.

[73] Florian Mock, Fleming Kretschmer, Anton Kriese, Sebastian Böcker, and Manja Marz. Taxonomic classification of dna sequences beyond sequence similarity using deep neural networks. *Proceedings of the National Academy of Sciences*, 119(35):e2122636119, 2022.

[74] Adithya Murali, Aniruddha Bhargava, and Erik S Wright. Idtaxa: a novel approach for accurate taxonomic classification of microbiome sequences. *Microbiome*, 6:1–14, 2018.

[75] Fabiane M Nachtigall, Alfredo Pereira, Oleksandra S Trofymchuk, and Leonardo S Santos. Detection of sars-cov-2 in nasal swabs using maldi-ms. *Nature biotechnology*, 38(10):1168–1173, 2020.

[76] Saul B Needleman and Christian D Wunsch. A general method applicable to the search for similarities in the amino acid sequence of two proteins. *Journal of molecular biology*, 48(3):443–453, 1970.

[77] Mark EJ Newman. A measure of betweenness centrality based on random walks. *Social networks*, 27(1):39–54, 2005.

[78] Gherman Novakovsky, Nick Dexter, Maxwell W Libbrecht, Wyeth W Wasserman, and Sara Mostafavi. Obtaining genetics insights from deep learning via explainable artificial intelligence. *Nature Reviews Genetics*, 24(2):125–137, 2023.

[79] Rachid Ounit, Steve Wanamaker, Timothy J Close, and Stefano Lonardi. Clark: fast and accurate classification of metagenomic and genomic sequences using discriminative k-mers. *BMC genomics*, 16:1–13, 2015.

[80] Lawrence Page, Sergey Brin, Rajeev Motwani, and Terry Winograd. The pagerank citation ranking: Bringing order to the web. Technical Report 1999-66, Stanford InfoLab, November 1999. Previous number = SIDL-WP-1999-0120.

[81] Corey M Peak, Amy Wesolowski, Elisabeth zu Erbach-Schoenberg, Andrew J Tatem, Erik Wetter, Xin Lu, Daniel Power, Elaine Weidman-Grunewald, Sergio Ramos, Simon Moritz, et al. Population mobility reductions associated with travel restrictions during the ebola epidemic in sierra leone: use of mobile phone data. *International journal of epidemiology*, 47(5):1562–1570, 2018.

[82] Koen Peeters Grietens, Charlotte Gryseels, Susan Dierickx, Melanie Bannister-Tyrrell, Suzan Trienekens, Sam-bunny Uk, Pisen Phoeuk, Sokha Suon, Srun Set, René Gerrets, et al. Characterizing types of human mobility to inform differential and targeted malaria elimination strategies in northeast cambodia. *Scientific reports*, 5(1):16837, 2015.

[83] Desislava Petkova, John Novembre, and Matthew Stephens. Visualizing spatial population structure with estimated effective migration surfaces. *Nature genetics*, 48(1):94–100, 2016.

[84] Thai-Hoang Pham, Yue Qiu, Jucheng Zeng, Lei Xie, and Ping Zhang. A deep learning framework for high-throughput mechanism-driven phenotype compound screening and its application to covid-19 drug repurposing. *Nature machine intelligence*, 3(3):247–257, 2021.

[85] Chiara Poletto, Sandro Meloni, Vittoria Colizza, Yamir Moreno, and Alessandro Vespignani. Host mobility drives pathogen competition in spatially structured populations. *PLoS computational biology*, 9(8):e1003169, 2013.

[86] Chiara Poletto, Sandro Meloni, Ashleigh Van Metre, Vittoria Colizza, Yamir Moreno, and Alessandro Vespignani. Characterising two-pathogen competition in spatially structured environments. *Scientific reports*, 5(1):7895, 2015.

[87] Andrew Rambaut, Edward C Holmes, Áine O’Toole, Verity Hill, John T McCrone, Christopher Ruis, Louis Du Plessis, and Oliver G Pybus. A dynamic nomenclature proposal for sars-cov-2 lineages to assist genomic epidemiology. *Nature microbiology*, 5(11):1403–1407, 2020.

[88] Bharath Reddy and Richard Fields. Performance analysis of multiple sequence alignment tools. In *Proceedings of the 2024 ACM Southeast Conference*, pages 167–174, 2024.

[89] Gesine Reinert, David Chew, Fengzhu Sun, and Michael S Waterman. Alignment-free sequence comparison (i): statistics and power. *Journal of Computational Biology*, 16(12):1615–1634, 2009.

[90] Rebecca J Rockett, Alicia Arnott, Connie Lam, Rosemarie Sadsad, Verlaine Timms, Karen-Ann Gray, John-Sebastian Eden, Sheryl Chang, Mailie Gall, Jenny Draper, et al. Revealing covid-19 transmission in australia by sars-cov-2 genome sequencing and agent-based modeling. *Nature medicine*, 26(9):1398–1404, 2020.

[91] Jason Rosado, Stéphane Pelleau, Charlotte Cockram, Sarah Hélène Merkling, Narimane Nekkab, Caroline Demeret, Annalisa Meola, Solen Kerneis, Benjamin Terrier, Samira Fafi-Kremer, et al. Multiplex assays for the identification of serological signatures of sars-cov-2 infection: an antibody-based diagnostic and machine learning study. *The Lancet Microbe*, 2(2):e60–e69, 2021.

[92] Nina Schwalbe and Brian Wahl. Artificial intelligence and the future of global health. *The Lancet*, 395(10236):1579–1586, 2020.

[93] Scott Schwartz, W James Kent, Arian Smit, Zheng Zhang, Robert Baertsch, Ross C Hardison, David Haussler, and Webb Miller. Human–mouse alignments with blastz. *Genome research*, 13(1):103–107, 2003.

[94] Samuel K Sheppard, David S Guttman, and J Ross Fitzgerald. Population genomics of bacterial host adaptation. *Nature Reviews Genetics*, 19(9):549–565, 2018.

[95] Fabian Sievers, Andreas Wilm, David Dineen, Toby J Gibson, Kevin Karplus, Weizhong Li, Rodrigo Lopez, Hamish McWilliam, Michael Remmert, Johannes Söding, et al. Fast, scalable generation of high-quality protein multiple sequence alignments using clustal omega. *Molecular systems biology*, 7(1):539, 2011.

[96] Temple F Smith, Michael S Waterman, et al. Identification of common molecular subsequences. *Journal of molecular biology*, 147(1):195–197, 1981.

[97] Ardi Tampuu, Zurab Bzhalava, Joakim Dillner, and Raul Vicente. Viraminer: Deep learning on raw dna sequences for identifying viral genomes in human samples. *PloS one*, 14(9):e0222271, 2019.

[98] Hourriyah Tegally, Eduan Wilkinson, Richard J Lessells, Jennifer Giandhari, Sureshnee Pillay, Nokukhanya Msomi, Koleka Mlisana, Jinal N Bhiman, Anne von Gottberg, Sibongile Walaza, et al. Sixteen novel lineages of sars-cov-2 in south africa. *Nature medicine*, 27(3):440–446, 2021.

[99] Julie D Thompson, Desmond G Higgins, and Toby J Gibson. Clustal w: improving the sensitivity of progressive multiple sequence alignment through sequence weighting, position-specific gap penalties and weight matrix choice. *Nucleic acids research*, 22(22):4673–4680, 1994.

- [100] Igor Ulitsky. Evolution to the rescue: using comparative genomics to understand long non-coding rnas. *Nature Reviews Genetics*, 17(10):601–614, 2016.
- [101] Ashish Vaswani, Noam Shazeer, Niki Parmar, Jakob Uszkoreit, Llion Jones, Aidan N Gomez, Łukasz Kaiser, and Illia Polosukhin. Attention is all you need. In *Advances in neural information processing systems*, pages 5998–6008, 2017.
- [102] Susana Vinga and Jonas Almeida. Alignment-free sequence comparison—a review. *Bioinformatics*, 19(4):513–523, 2003.
- [103] Lin Wan, Gesine Reinert, Fengzhu Sun, and Michael S Waterman. Alignment-free sequence comparison (ii): theoretical power of comparison statistics. *Journal of Computational Biology*, 17(11):1467–1490, 2010.
- [104] Guangyu Wang, Xiaohong Liu, Kai Wang, Yuanxu Gao, Gen Li, Daniel T Baptista-Hon, Xiaohong Helena Yang, Kanmin Xue, Wa Hou Tai, Zeyu Jiang, et al. Deep-learning-enabled protein–protein interaction analysis for prediction of sars-cov-2 infectivity and variant evolution. *Nature Medicine*, 29(8):2007–2018, 2023.
- [105] Nicole L Washington, Karthik Gangavarapu, Mark Zeller, Alexandre Bolze, Elizabeth T Cirulli, Kelly M Schiabor Barrett, Brendan B Larsen, Catelyn Anderson, Simon White, Tyler Cassens, et al. Emergence and rapid transmission of sars-cov-2 b. 1.1. 7 in the united states. *Cell*, 184(10):2587–2594, 2021.
- [106] Gregory A Wellenius, Swapnil Vispute, Valeria Espinosa, Alex Fabrikant, Thomas C Tsai, Jonathan Hennessy, Andrew Dai, Brian Williams, Krishna Gadepalli, Adam Boulanger, et al. Impacts of social distancing policies on mobility and covid-19 case growth in the us. *Nature communications*, 12(1):3118, 2021.
- [107] Amy Wesolowski, Taimur Qureshi, Maciej F Boni, Pål Roe Sundsøy, Michael A Johansson, Syed Basit Rasheed, Kenth Engø-Monsen, and Caroline O Buckee. Impact of human mobility on the emergence of dengue epidemics in pakistan. *Proceedings of the national academy of sciences*, 112(38):11887–11892, 2015.
- [108] Jochen BW Wolf and Hans Ellegren. Making sense of genomic islands of differentiation in light of speciation. *Nature Reviews Genetics*, 18(2):87–100, 2017.
- [109] He S Yang, Yu Hou, Ljiljana V Vasovic, Peter AD Steel, Amy Chadburn, Sabrina E Racine-Brzostek, Priya Velu, Melissa M Cushing, Massimo Loda, Rainu Kaushal, et al. Routine laboratory blood tests predict sars-cov-2 infection using machine learning. *Clinical chemistry*, 66(11):1396–1404, 2020.
- [110] Jaewon Yang, Julian McAuley, and Jure Leskovec. Community detection in networks with node attributes. In *2013 IEEE 13th International Conference on Data Mining*, pages 1151–1156, 2013.
- [111] Yang Yang, Katherine E Niehaus, Timothy M Walker, Zamin Iqbal, A Sarah Walker, Daniel J Wilson, Tim EA Peto, Derrick W Crook, E Grace Smith, Tingting Zhu, et al. Machine learning for classifying tuberculosis drug-resistance from dna sequencing data. *Bioinformatics*, 34(10):1666–1671, 2018.
- [112] Manzil Zaheer, Guru Guruganesh, Kumar Avinava Dubey, Joshua Ainslie, Chris Alberti, Santiago Ontanon, Philip Pham, Anirudh Ravula, Qifan Wang, Li Yang, et al. Big bird: Transformers for longer sequences. In *NeurIPS*, 2020.
- [113] Qian Zhang, Kaiyuan Sun, Matteo Chinazzi, Ana Pastore y Piontti, Natalie E Dean, Diana Patricia Rojas, Stefano Merler, Dina Mistry, Piero Poletti, Luca Rossi, et al. Spread of zika virus in the americas. *Proceedings of the national academy of sciences*, 114(22):E4334–E4343, 2017.
- [114] Hong Zhou, Jingkai Ji, Xing Chen, Yuhai Bi, Juan Li, Qihui Wang, Tao Hu, Hao Song, Runchu Zhao, Yanhua Chen, et al. Identification of novel bat coronaviruses sheds light on the evolutionary origins of sars-cov-2 and related viruses. *Cell*, 184(17):4380–4391, 2021.
- [115] Jian Zhou and Olga G Troyanskaya. Predicting effects of noncoding variants with deep learning–based sequence model. *Nature methods*, 12(10):931–934, 2015.
- [116] Andrzej Zielezinski, Susana Vinga, Jonas Almeida, and Wojciech M Karlowski. Alignment-free sequence comparison: benefits, applications, and tools. *Genome biology*, 18(1):1–17, 2017.

5 Supplementary Methods and Extended Results

We included additional experimental results to further validate the robustness of the proposed Genome Misclassification Network Analysis (GMNA) framework. These experiments involved different AI accuracy levels and experimental setups, including soft and hard misclassification, as well as misclassification under the LOCO setup, to assess the consistency of the framework’s results under diverse conditions.

In Fig. 9, we observed spatial dependencies among COVID-19 genomes from neighboring regions, consistent with our previous findings. However, in this setting, with the higher prediction accuracy of 74.12% under MCC, and 72.78% under the LOCO setup, the spatial dependencies were confined to Europe and North America, where sufficient misclassifications were available for correlation analysis.

Unlike in Fig. 3 where the classification accuracy is lower at 58.02% and in Fig. 8 at 60.88%, more misclassified instances were resulted from the less accurate classifier and gave us more instances for correlational analysis on genome ensemble association at a global scope.

These supplementary results confirm that while higher prediction accuracy reduces the number of misclassified instances available for correlation analysis, the GMNA framework remains effective in detecting region-specific dependencies when sufficient data are available. This demonstrates the flexibility of the framework to adapt to AI's with varying accuracy while still providing meaningful insights into the spatial associations of COVID-19 genome sequences.

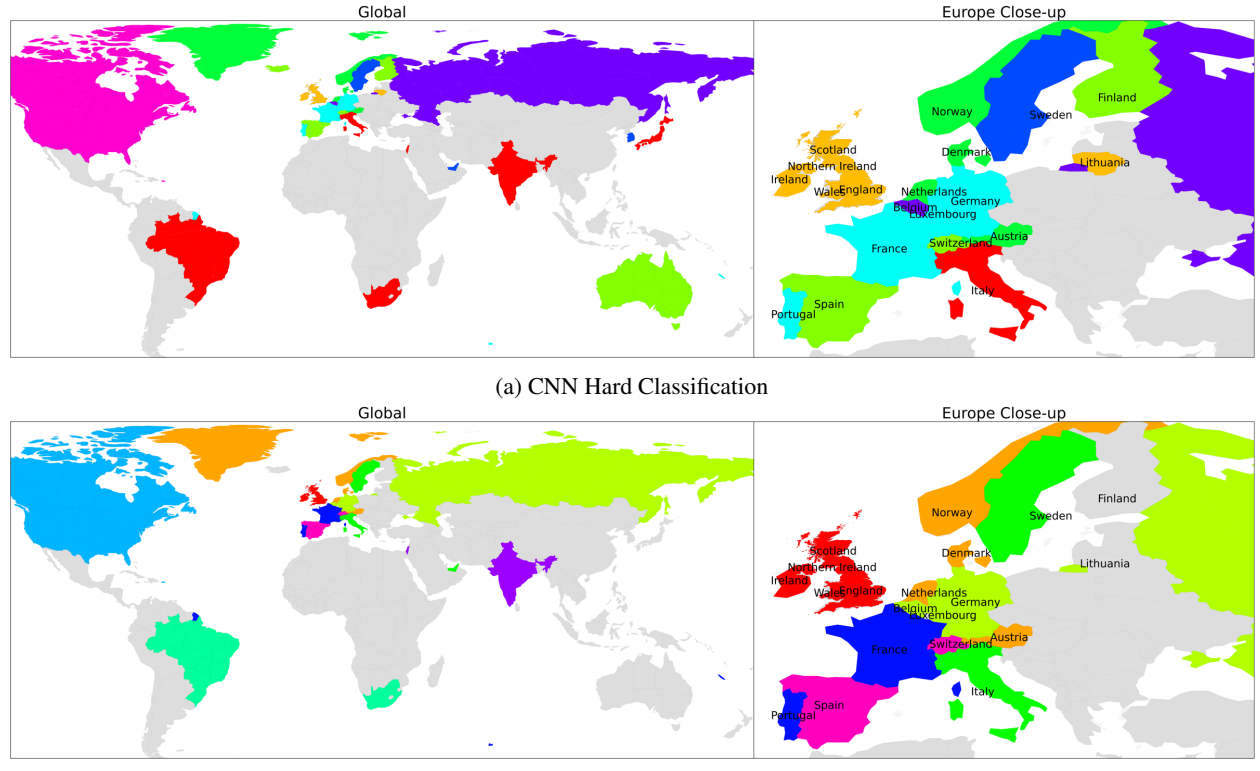
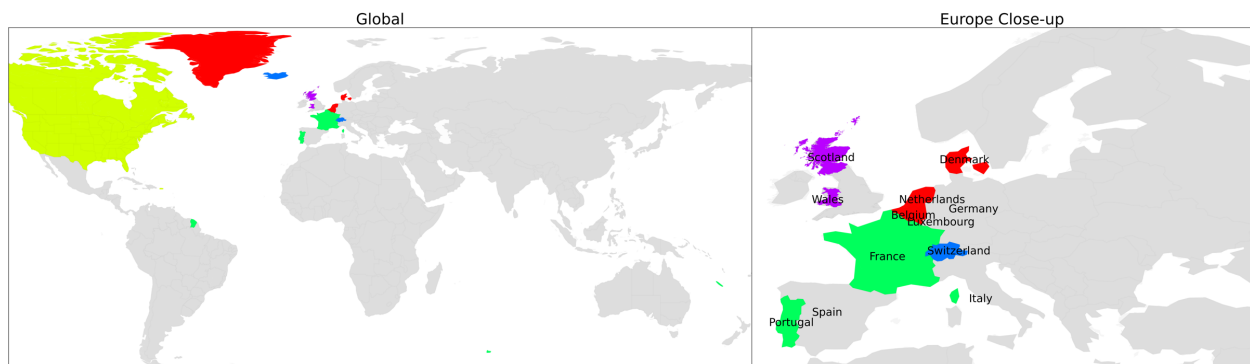


Figure 8: Multiclass CNN Misclassification Network: Clustering results on the misclassification network from a convolutional neural network classifier with a sampling threshold=sample size=1000.



(a) LOCO Multiclass CNN Soft Misclassification Network: Clustering results on the soft misclassification network from a CNN LOCO classifier with a sampling threshold=sample size=3000.



(b) Multiclass CNN Soft Misclassification Network: Clustering results on the soft misclassification network from a CNN classifier with a sampling threshold=sample size=3000.

Figure 9: Multiclass CNN Soft Misclassification Network: Clustering results on the soft misclassification network from a convolutional neural network classifier with a sampling threshold=sample size=3000.